

Total transmission and total reflection of acoustic wave by zero index metamaterials loaded with general solid defects

Ziyu Wang,^{1,2,3} Fan Yang,³ LiBing Liu,³ Ming Kang,³ and Fengming Liu^{1,a)}

¹School of Science, Hubei University of Technology, Wuhan 430068, China

²School of Physics and Technology, Wuhan University, Wuhan 430072, China

³Materials and Technology Institute, Dongfeng Motor, Wuhan 430056, China

PACS 47.35.Rs - Sound waves

PACS 62.30.+d - Mechanical and elastic waves; vibrations

Abstract:

This work investigates acoustic wave transmission property through a zero index metamaterials (ZIM) waveguide embedded with a general solid defect. Total transmission and total reflection can be achieved by adjusting the parameters of the solid defect. Compared to the previous study of liquid defects, our work comprehensively studies how transverse wave speed of the solid defect affects the acoustic wave propagation through the waveguide. The necessary condition of realizing total reflection by tailoring transverse wave speed is given. Thus, our work provides more possibilities to manipulate acoustic wave propagation through ZIM.

^{a)} E-mail: fmliu@hbut.edu.cn

Zero index metamaterials (ZIM), whose permittivity and permeability are simultaneously or individually near zero, have been studied both theoretically and experimentally and showed many intriguing properties[1-12]. Enoch *et al.* [2] showed that ZIM can be used to enhance the directive emission of an embedded source; Silveirinha and Engheta [3] presented an epsilon-near-zero (ENZ) medium that can “squeeze” electromagnetic (EM) wave through a very narrow channel, which has been demonstrated experimentally [4, 5]. Hao *et al.* [8] first showed that total reflection or total transmission can be realized by introducing perfect electric (magnetic) conductor defects into the ZIM waveguide. Then, several works follow which concern manipulating EM wave propagation through ZIM waveguide by tailoring the parameters of the dielectric defect [9-12]. Meanwhile, acoustic metamaterials have also stirred considerable excitement for they can be engineered to exhibit intriguing physical phenomena [13-23]. Past efforts focused on realizing acoustic metamaterials exhibiting effectively negative bulk modulus and negative mass density [13-16]. Recently, acoustic ZIM has drawn intense attention from several research groups [17-23]. Among them, Qi *et al.* [23] introduced various kinds of defects in order to control acoustic wave transmission through the acoustic ZIM waveguide structure. However, they have only considered the liquid and ideal rigid defects. General solid defects, which are more complicated because of the co-existence of longitudinal and transverse waves, still need further research.

In this work, we investigate the acoustic wave transmission through the ZIM waveguide embedded with general solid defects. Comprehensive analysis of how the

transverse wave speed of the solid defects affects the transmission is provided, and numerical simulations are then carried out to testify our theory. In contrast to liquid defects, general solid defects provide more tunable parameters to control the transmission of acoustic wave through ZIM waveguide.

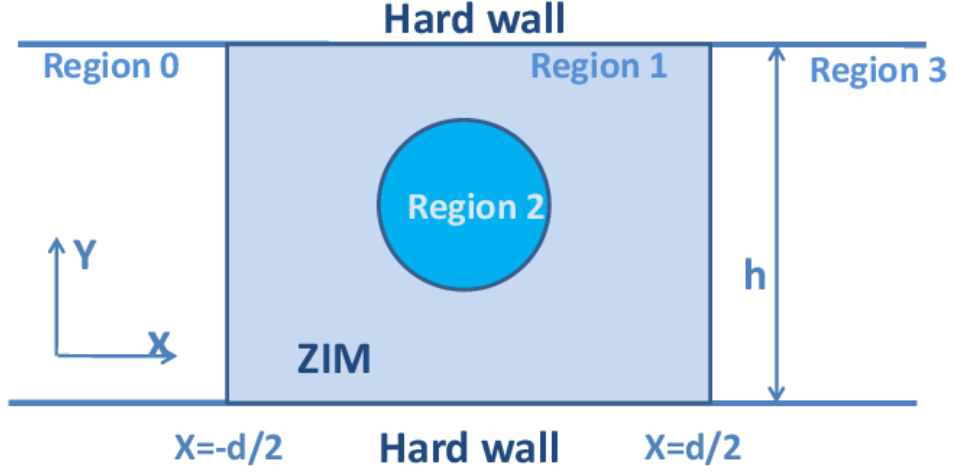


Fig. 1: (Colour on-line) Schematic of the 2D waveguide structure with water (region 0 and 3), ZIM (region 1), and an embedded defect (region 2).

A two-dimensional acoustic waveguide structure, which consists of four distinct regions, is illustrated in Fig.1. The regions 0 and 3 filled with water (with mass density ρ_0 , bulk modulus κ_0 and speed $c_0 = \sqrt{\kappa_0/\rho_0}$) are separated by acoustic ZIM (region 1) with effective mass density ρ_1 and effective bulk modulus κ_1 . And a cylindrical solid defect (region 2) with radius a , mass density ρ_2 , bulk modulus κ_2 , and shear modulus μ_2 is embedded in the ZIM region. The walls of the waveguide are set to be hard walls.

Suppose that a plane harmonic acoustic wave $P_{inc} = Pe^{i(k_0x - \omega t)}$ is incident from left to right inside the waveguide, where P is the amplitude of the incident field, k_0 is the wave vector in the regions 0 and ω is the angular frequency. We omit the time

variation item in the rest of this paper for convenience. Thus, the pressure and velocity fields in the region 0 can be written as

$$P_0 = P[e^{ik_0(x+d/2)} + Re^{-ik_0(x+d/2)}], v_0 = [e^{ik_0(x+d/2)} - Re^{-ik_0(x+d/2)}]P/\eta_0, \quad (1)$$

while in region 3 the pressure and velocity fields must have the form

$$P_3 = TP e^{ik_0(x-d/2)}, v_3 = e^{ik_0(x-d/2)} PT/\eta_0, \quad (2)$$

where R and T are the reflection and transmission coefficients and $\eta_0 = \sqrt{\rho_0 \kappa_0}$ is the impedance of the water host. In region 1, the pressure and velocity fields are presented by P_1 and $v_1 = (1/i\omega\rho_1)\nabla P_1$, respectively. In the limit $\rho_1 \approx 0$, the pressure field P_1 must be constant in the ZIM so as to keep v_1 as finite value. Then by using the continuous boundary condition at $x = -d/2$ and $x = d/2$, we have $P(1+R) = P_1$ and $TP = P_1$, which leads to $1+R = T$. Applying the law of conservation of mass $\oint \rho v_r dl = \int (\rho/\kappa)(\partial p/\partial t) ds$ (v_r denotes the normal component of the velocity field), we can find out the transmission coefficient of the waveguide as,

$$T = \frac{1}{1 - (\eta_0/2hp_1) \oint_{\partial A_2} v_{2r} dl}, \quad (3)$$

where ∂A_2 is the boundary of the defect and v_{2r} is the normal component of velocity field in the defect. For simplicity, only one defect is considered here. To evaluate T , we need to find the normal component of velocity field v_{2r} , which can be obtained by considering the elastic boundary conditions between the solid cylinder and the ZIM.

In region 2, the displacement fields are described by the elastic wave equation $(\lambda_2 + 2\mu_2)\nabla(\nabla \cdot \mathbf{u}_2) - \mu_2\nabla \times \nabla \times \mathbf{u}_2 + \rho_2\omega^2\mathbf{u}_2 = 0$, where \mathbf{u}_2 is the displacement field, μ_2 denotes shear modulus, and λ_2 represents the Lamé constant satisfying $\kappa_2 = \lambda_2 + \mu_2$.

We note that, in contrast to the liquid defects studied previously [23], another elastic

parameter μ_2 needs to be considered here. In cylindrical coordinates, the general solution in the cylinders can be expressed as

$$\mathbf{u}_2 = \sum_n [d_{n1} \mathbf{J}_{n1}(k_{2l}r) + d_{n2} \mathbf{J}_{n2}(k_{2l}r)], \quad (4)$$

where $\mathbf{J}_{n1}(k_{2l}r)$ and $\mathbf{J}_{n2}(k_{2l}r)$ are, respectively, defined as

$$\begin{aligned} \mathbf{J}_{n1}(k_{2l}r) &= \nabla [J_n(k_{2l}r)e^{in\phi}] \\ \mathbf{J}_{n2}(k_{2l}r) &= \nabla \times [\hat{\mathbf{z}} J_n(k_{2l}r)e^{in\phi}] \end{aligned}, \quad (5)$$

where $k_{2l} = \omega \sqrt{\rho_2 / (\kappa_2 + \mu_2)}$, $k_{2t} = \omega \sqrt{\rho_2 / \mu_2}$, $J_n(x)$ is the Bessel function and n is the angular quantum number. The elastic boundary conditions require that

$$\begin{aligned} u_{1r} \Big|_{r=a} &= u_{2r} \Big|_{r=a} \\ p_1 \Big|_{r=a} &= \tau_{2rr} \Big|_{r=a}, \\ 0 &= \tau_{2r\phi} \Big|_{r=a} \end{aligned}, \quad (6)$$

where u_r is the normal component of displacement, τ_{rr} is the normal projection of stress tensor, and $\tau_{r\phi}$ is the tangential projection of stress tensor. We note that, to satisfy the elastic boundary conditions, the angular quantum number n in Eq. (5) can only take 0 due to the fact that the pressure field P_1 is constant in the ZIM region.

The elastic boundary conditions lead to the following eqs.

$$\begin{aligned} u_{1r} &= D_{11}d_{01} + D_{12}d_{02} \\ p_1 &= D_{21}d_{01} + D_{22}d_{02}, \\ 0 &= D_{31}d_{01} + D_{32}d_{02} \end{aligned}, \quad (7)$$

where $D_{12} = D_{22} = D_{31} = 0$, $D_{11} = -k_{2l} J_1(k_{2l}a)$, $D_{32} = -k_{2t}^2 J_1(k_{2l}a)$, and $D_{21} = -2(\mu_2 + \lambda_2)k_{2l} J_1(k_{2l}a)/a + (\lambda_2 + 2\mu_2)k_{2l}^2 J_2(k_{2l}a)$ while n takes 0. By solving Eq.

(7), we obtain $u_{1r} = u_{2r} = \frac{D_{11}}{D_{21}} p_1$. Then, as the velocity field is the derivative of the

displacement field with respect to time, we have $v_{2r} = \frac{\omega}{i} u_{2r} = \frac{\omega}{i} \frac{D_{11}}{D_{21}} p_1$. Finally, the

transmission coefficient (Eq. (3)) can be expressed as

$$T = \frac{1}{1 + \frac{\omega\eta_0\pi ak_{2l}J_1(k_{2l}a)}{ihD_{21}}}. \quad (8)$$

A deep inspection of Eq. (8) shows the transmission characteristics of the system. First, we can see that total transmission arises if $D_{11} = 0$, i.e. $J_1(k_{2l}a) = 0$. As is noted if the longitudinal wave speed is fixed and makes $J_1(k_{2l}a) = 0$, whatever value the shear modulus μ_2 appearing in D_{21} takes will not change the total transmission. To verify the analysis, numerical simulations are carried out by using the finite element method (FEM). We set $d = h = 1.4\text{m}$. The wavelength λ_0 of the incident wave is 0.55m . The ZIM with $\rho_1 = 0.0001\rho_0$ and $1/\kappa_1 = 0.0001(1/\kappa_0)$ is impedance match to water. We fix the radius $a = 0.49\text{m}$ and mass density $\rho_2 = 2\rho_0$ for all the cases considered. To satisfy $J_1(k_{2l}a) = 0$, a solid defect with fixed $c_{2l} = 1.4604c_0$ and tunable transverse wave speed is considered. Fig. 2(a) shows the transmission coefficients as a function of the transverse wave speed of the solid defect. The variation range of the transverse wave speed is restricted by the condition $\sqrt{2}c_{2t} < c_{2l}$. It can be seen that $T=1$ for arbitrary value of the transverse wave speed, which indicates adjusting the transverse wave speed does not change total transmission. Although the divergence of D_{21} can also lead to $T=1$, tailoring μ_2 cannot make D_{21} diverge obviously considering the expression of D_{21} . Therefore, total transmission cannot be achieved by tailoring the transverse wave speed. In Fig. 2(b), we show the pressure field distribution of the ZIM waveguides embedded with the solid defect (with $c_{2l} = 1.4604c_0$ and $c_{2t} = 0.7181c_0$). The plot clearly demonstrates total transmission of the incident radiation. We would like to remark that as long as the longitudinal wave speed of the

defect is fast enough, $J_1(k_{2t}a)$ will approach zero and thus total transmission happens, which is just like the case of ideal rigid defect [23].

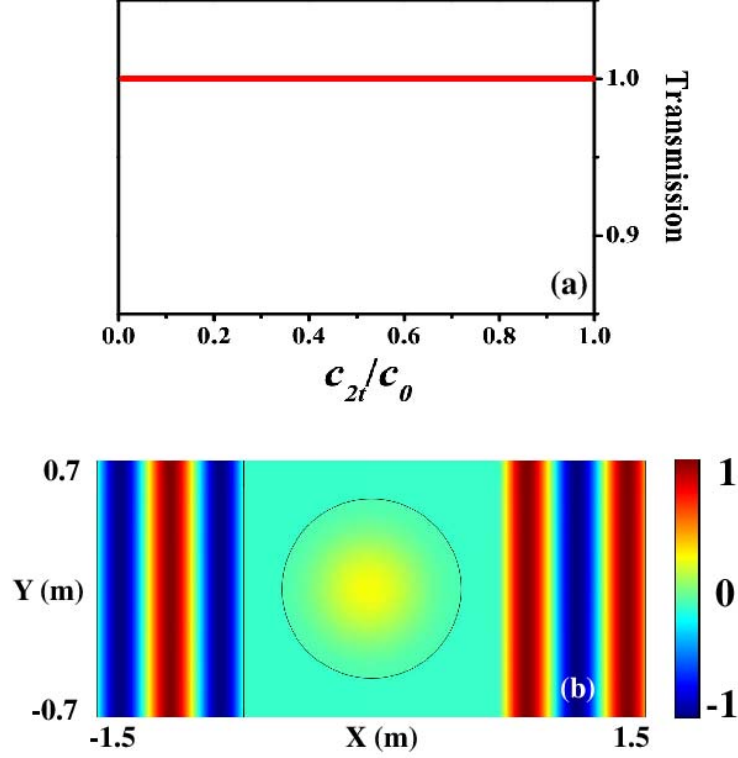


Fig. 2: (Colour on-line) (a) Transmission coefficients as a function of the transverse wave speed of the solid defect with fixed $c_{2l} = 1.4604c_0$. (b) The pressure field distributions of total transmission for the solid defect with $c_{2l} = 1.4604c_0$ and $c_{2t} = 0.7181c_0$.

Next, we will discuss whether tailoring the transverse wave speed can be used to achieve total reflection. From Eq. (8), we see that if $J_1(k_{2t}a) \neq 0$ and $D_{21} = 0$, then $T=0$, in which case total reflection happens. Further, the expression of D_{21} reveals that $J_1(k_{2t}a)$ and $J_2(k_{2t}a)$ should have the same sign to guarantee that D_{21} has the possibility of equaling zero. Therefore, the necessary condition to realize total reflection by tailoring transverse wave speed is $J_1(k_{2t}a) \neq 0$ and $J_1(k_{2t}a) \times J_2(k_{2t}a) > 0$.

We consider a solid defect with fixed $c_{2t} = 2.6846c_0$, which is chosen to satisfy $J_1(k_{2t}a) \neq 0$ and $J_1(k_{2t}a) \times J_2(k_{2t}a) > 0$, and tunable transverse wave speed. Fig. 3(a) shows the transmission coefficients as a function of the transverse wave speed of the solid defect. It can be found that $T=0$ at $c_{2t} = 1.5208c_0$. And by using the expression of D_{21} , we find $D_{21} = 0$ at $c_{2t} = 1.5215c_0$. The simulated result agrees well with the theoretic result. According to Eq. (7), $D_{21} = 0$ means that the normal projection of stress tensor is zero at the interface of the defect. Imposed by the elastic boundary condition, P_1 should be zero anywhere as P_1 is constant in the region (1). Thus, the incident wave will be totally blocked, which indicates total reflection. In Fig. 3(b), we show the pressure field distribution of the ZIM waveguides as the total reflection happens. As expected, one can see that the pressure field P_1 disappears inside region (1) and the normal projection of stress tensor is zero at the interface indeed.

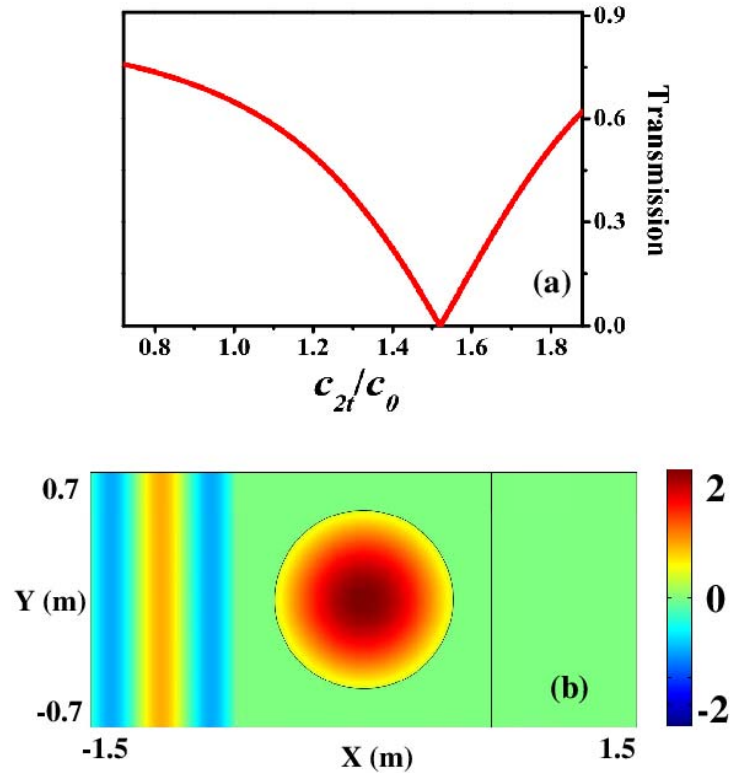


Fig. 3: (Colour on-line) (a) Transmission coefficients as a function of the transverse wave speed of the solid defect with fixed $c_{2l} = 2.6846c_0$. (b) The pressure field distributions of total reflection for the solid defect with $c_{2l} = 2.6846c_0$ and $c_{2t} = 1.5208c_0$.

We would like to mention that it is impossible to achieve total reflection by tailoring the transverse wave speed if $J_1(k_{2l}a) \times J_2(k_{2l}a) < 0$. In Fig. 4, we show the transmission coefficients as a function of the transverse wave speed of a solid defect with $c_{2l} = 1.1409c_0$, which is chosen to satisfy $J_1(k_{2l}a) \times J_2(k_{2l}a) < 0$. It can be observed that no total reflection happens in such condition.

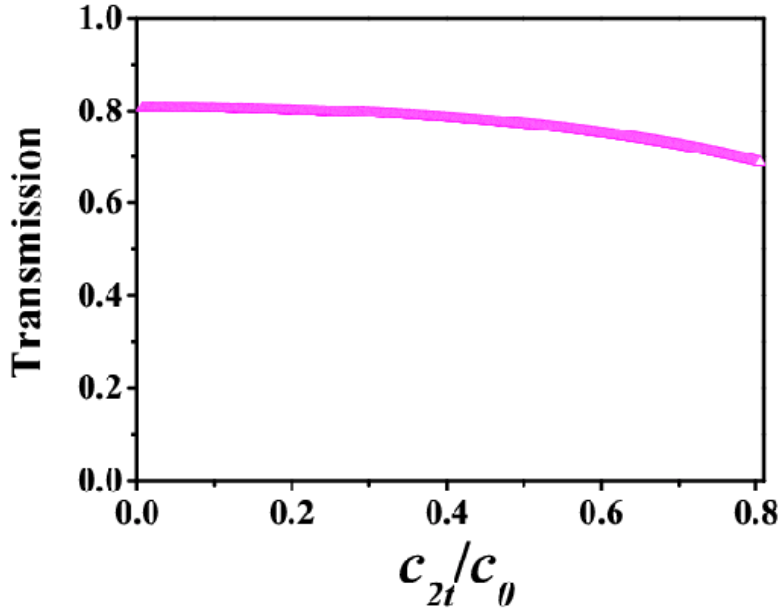


Fig. 4: (Colour on-line) Transmission coefficients as a function of the transverse wave speed of the solid defect with fixed $c_{2l} = 1.1409c_0$.

In conclusion, we have demonstrated how to achieve total reflection and total transmission of acoustic waves by embedding a general solid defect in the ZIM waveguide. Theoretical analysis shows that adjusting transverse wave speed can only

be applied to achieve total reflection instead of total transmission. Numerical simulations confirm our theory. We would like to point out that our result can be extended to the ZIM waveguide embedded with multiple defects and the tunable solid defects can be made of polymeric materials. Our work provides more choices for manipulating acoustic wave propagation in ZIM with embedded general solid defects.

The author acknowledges helpful discussions with Prof. Zhengyou Liu.

References:

1. Ziolkowski R. W., *Phys. Rev. E*, **70** (2004) 046608.
2. Enoch S., Tayeb G., Sabouroux P., Guerin N. and Vincent P., *Phys. Rev. Lett.*, **89** (2002) 213902.
3. Silveirinha M. G. and Engheta N., *Phys. Rev. Lett.*, **97** (2006) 157403.
4. Liu R. P., Cheng Q., Hand T., Mock J. J., Cui T. J., Cummer S. A. and Smith D. R., *Phys. Rev. Lett.*, **100** (2008) 023903.
5. Edwards B., Alù A., Young M. E., Silveirinha M. and Engheta N., *Phys. Rev. Lett.*, **100** (2008) 033903.
6. Wang Fan and Chan C. T., *Europhys. Lett.*, **99** (2012) 67002.
7. Yuan Y., Wang N. and Lim J. H., *Europhys. Lett.*, **100** (2012) 34005.
8. Hao J., Yan W. and Qiu M., *Appl. Phys. Lett.*, **96** (2010) 101109.

9. Nguyen V. C., Chen L. and Halterman K., *Phys. Rev. Lett.*, **105** (2010) 233908.
10. Xu Y. and Chen H., *Appl. Phys. Lett.* **98** (2011) 113501.
11. Luo J., Xu P., Chen H., Ho B., Gao L. and Lai Y., *Appl. Phys. Lett.*, **100** (2012) 221903.
12. Wu Ying and Li Jichun, *Appl. Phys. Lett.*, **102** (2013) 183105.
13. Liu Z., Zhang X., Mao Y., Zhu Y. Y., Yang Z., Chan C. T. and Sheng P., *Science*, **289** (2000) 1734.
14. Li J. and Chan C. T., *Phys. Rev. E*, **70** (2004) 055602(R).
15. Fang N., Xi D., Xu J., Ambati M., Srituravanich W., Sun C. and Zhang X., *Nature Mater.*, **5** (2006) 452.
16. Graciá-Salgado R., Torrent D. and Sánchez-Dehesa J., *New J. Phys.*, **14** (2012)103052.
17. Bongard F., Lissek H. and Mosig J. R., *Phys. Rev. B*, **82** (2010) 094306.
18. Liu F., Huang X. and Chan C. T., *Appl. Phys. Lett.*, **100** (2012) 071911.
19. Liang Z. and Li J., *Phys. Rev. Lett.*, **108** (2012) 114301.
20. Xie Yangbo, Popa Bogdan-Ioan, Zigoneanu Lucian and Cummer Steven A., *Phys. Rev. Lett.*, **110** (2013) 175501.
21. Park Jong Jin, Lee K. J. B., Wright Oliver B., Jung Myoung Ki and Lee Sam H., *Phys. Rev. Lett.*, **110** (2013) 244302.
22. Park Choon Mahn and Lee Sang Hun, *Appl. Phys. Lett.*, **102** (2013) 241906.
23. Wei Q., Cheng Y. and Liu X. J., *Appl. Phys. Lett.*, **102** (2013) 174104.